General approach to the quantum kicked particle in a magnetic field:
Quantum-antiresonance transition

Itzhack Dana[1] and Dmitry L. Dorofeev[1,2]

[1]*Minerva Center and Department of Physics, Bar-Ilan University, Ramat-Gan 52900, Israel*
[2]*Department of Physics, Voronezh State University, Voronezh 394693, Russia*

The quantum kicked particle in a magnetic field is studied in a weak-chaos regime under realistic conditions, i.e., for *general* values of the conserved coordinate x_c of the cyclotron orbit center. The system exhibits spectral structures ["Hofstadter butterflies" (HBs)] and quantum diffusion depending sensitively on x_c. Most significant changes take place when x_c approaches the value at which quantum antiresonance (exactly periodic recurrences) can occur: the HB essentially "doubles" and the quantum-diffusion coefficient $D(x_c)$ is strongly reduced. An explanation of these phenomena, including an approximate formula for $D(x_c)$ in a class of wave packets, is given on the basis of an effective Hamiltonian which is derived as a power expansion in a small parameter. The global quantum diffusion of a two-dimensional wave packet for all x_c is briefly considered.

PACS number(s): 05.45.Mt, 05.45.Ac, 03.65.−w

I. INTRODUCTION

Simple quantum systems whose classical counterparts are nonintegrable exhibit a variety of remarkable phenomena [1] which continue to attract much interest in several contexts. A realistic system, whose experimental realization by different methods has been the object of many recent works (see a very partial list in Ref. [2]), is the well-known kicked rotor [1,3,4], modeling the dynamical-localization phenomenon. A class of systems exhibiting basically different phenomena, such as quantum diffusion associated with a fractal spectrum, are represented by Hamiltonians periodic in phase space [5–20]. The simplest such system is the integrable Harper model [5] with Hamiltonian $H=\cos(x)+\cos(p)$, whose quantization describes the energy spectrum within a Bloch band in a magnetic field or within a broadened Landau level in a crystalline periodic potential [5–7,10]. Plotting this spectrum as a function of the magnetic flux through a unit cell (this flux is related to a scaled Planck constant for the Harper model) gives the well-known "Hofstadter butterfly" [6], featuring a clearly fractal structure [9]. Quite recently [10], much of this structure was detected experimentally.

The simplest nonintegrable system with a mixed phase space and a periodic Hamiltonian is the kicked Harper model (KHM) [11–19] with $H=\cos(p)+\cos(x)\Sigma_{s=-\infty}^{\infty}\delta(t/T-s)$, which reduces to the Harper Hamiltonian when the time period $T\to 0$. The KHM models the regular-chaotic transition [11,19] as well as the effect of chaos on a fractal spectrum and on quantum diffusion [13]. It seems that the only realistic interpretation of the KHM is its exact relation [16] with a particular case of the two-dimensional (2D) system of the periodically kicked particle in a magnetic field [21–23]. This system is described by

$$H = \Pi^2/2 - K\cos(x)\sum_{s=-\infty}^{\infty}\delta(t-sT), \qquad (1)$$

where $\mathbf{\Pi}=(\Pi_x,\Pi_y)=\mathbf{p}-\mathbf{B}\times\mathbf{r}/(2c)$ is the kinetic momentum of a particle with unit charge and unit mass in a uniform magnetic field **B** (along the z axis) and K is a nonintegrability parameter. Let us first summarize some known facts about (1) [21–23]. It is crucial to represent (1) in the natural degrees of freedom in a magnetic field, given by the independent conjugate pairs (Π_x,Π_y) and (x_c,y_c) (coordinates of the center of a cyclotron orbit) [24]. Defining $u=\Pi_x/\omega$, $v=\Pi_y/\omega$, where $\omega=B/c$ is the cyclotron frequency, and using the relation $x_c=x+\Pi_y/\omega=x+v$ (from simple geometry), (1) can be rewritten as follows [22]:

$$H = \omega^2(u^2+v^2)/2 - K\cos(x_c-v)\sum_{s=-\infty}^{\infty}\delta(t-sT). \qquad (2)$$

Since y_c does not appear in (2), its conjugate mate x_c is *conserved* and, therefore, can be treated as a parameter. This reduces (1) to an ensemble of periodically kicked harmonic oscillators parametrized by x_c. Classically, these degenerate systems are expected to exhibit unbounded chaotic diffusion in the (u,v) phase plane for arbitrarily small values of K, especially under resonance conditions, with $\alpha\equiv\omega T$ a rational multiple of 2π [21,22]; this diffusion is observed to take place on a "stochastic web" whose symmetry depends on α. Examples of square-symmetry webs ($\alpha=\pi/2$) are shown in Fig. 1. The KHM is exactly related to (2), in essence, only for $\alpha=\pi/2$ and for *very special* values of x_c, $x_c=0$, π (see Sec. A 1 of the Appendix and generalizations of this relation in Refs. [15,16]). Now, the classical properties of (2), in particular the structure of the stochastic web, its width, and
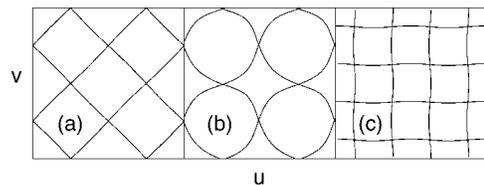

FIG. 1. Classical stochastic webs for $K=0.157$ and $\alpha=\pi/2$, generated by the map (8) in three cases: (a) $x_c=0$; (b) $x_c=1.47$; (c) $x_c=\pi/2$. The range of both u and v in all the plots is $[-2\pi,2\pi]$.

−the diffusion rate on it, are known to depend *strongly* on x_c [22,23] (see also Sec. III). In addition, one should notice that *realistic* classical ensembles or 2D wave packets for (1) exhibit *all* values of x_c. These facts motivate the investigation of the quantum properties of (2) for arbitrary x_c. Except for general results [15,16], these properties appear to be essentially unexplored.

In this paper, we present a study of the quantized system (2) for general x_c. We focus on the weak-chaos regime of small K and, as in the classical studies [22,23], on the case of $\alpha = \pi/2$. The global spectral features of the system at fixed x_c are exhibited by a suitably defined plot of the quasienergy spectrum as a function of a scaled Planck constant $\hbar$. The term Hofstadter butterfly (HB) is extended so as to refer to such a plot. The quantum properties are found to depend sensitively on x_c. Most significant changes take place when x_c approaches the value of $\pi/2$ at which quantum antiresonance (QAR), i.e., exactly periodic recurrences [15,25], occurs for integer $\hbar/(2\pi)$. While the HB for most values of x_c is approximately the standard one of the Harper model [6], the HB for $x_c = \pi/2$ is, up to a local scaling, a perturbed "doubled" version of the standard HB. This change of the HB structure in the "QAR transition" $x_c \to \pi/2$ is explained on the basis of an effective Hamiltonian which is derived as a power expansion in a small parameter. For irrational $\hbar/(2\pi)$, the time evolution of wave packets is observed to exhibit approximately an asymptotic quantum diffusion. This is characterized by either a diffusion coefficient $D(x_c)$ at fixed x_c or a global coefficient $\bar{D}$, given by a weighted average of $D(x_c)$ over x_c. An approximate formula for $D(x_c)$ in a simple class of wave packets is derived from the effective Hamiltonian and is verified numerically. As $x_c \to \pi/2$, $D(x_c)$ decreases and QAR is manifested by the fact that $D(\pi/2)$ is significantly smaller than typical values of $D(x_c)$. While these phenomena are of a purely quantum nature, they have classical analogs. The paper is organized as follows. In Sec. II, we recall the QAR phenomenon [15,25] and study general spectral properties of the system (2), also on the basis of an effective Hamiltonian which is derived as an expansion in a small parameter. In Sec. III, we consider classical limits and analogs of some of the results in Sec. II. In Sec. IV, we study the quantum diffusion of wave packets for general x_c, using also the effective-Hamiltonian approximation. A summary and conclusions are presented in Sec. V. Proofs of several statements in Secs. I, II, and IV are given in the Appendix.

II. QUANTUM ANTIRESONANCE, GENERAL SPECTRAL PROPERTIES, AND EFFECTIVE HAMILTONIAN

To quantize the system (2), (u,v) are replaced by the corresponding conjugate operators $(\hat{u},\hat{v})$. From the definitions $u = \Pi_x/\omega$, $v = \Pi_y/\omega$, where $(\Pi_x, \Pi_y) = \mathbf{p} - \mathbf{B} \times \mathbf{r}/(2c)$ and $\omega = B/c$, it is easy to see that $(\hat{u},\hat{v})$ satisfy $[\hat{u},\hat{v}] = i\hbar/\omega$. We choose units such that $\omega = 1$, so that $[\hat{u},\hat{v}] = i\hbar$, where $\hbar$ is a scaled Planck constant. The one-period evolution operator for the quantized system (2) will be denoted by $\hat{U}_T(x_c)$. Let us now recall the phenomenon of *quantum antiresonance* (QAR) [15]. Under classical resonance conditions, $\alpha = \omega T$

$= 2\pi j/l$ (j and l are coprime integers), QAR for the system (2) is defined by $\hat{U}_T^l(x_c) = $ constant phase factor, i.e., exactly periodic recurrences with the natural resonance period lT. As shown in Ref. [15], QAR occurs in the nonintegrable ($l > 2$) case of a general kicked harmonic oscillator only if three conditions are satisfied: (a) The kicking periodic potential is an *odd* function, up to an additive constant; this implies that $x_c = \pi/2$, $3\pi/2$ for the potential $\cos(x_c - v)$ in Eq. (2). (b) $l = 4$ or $l = 6$, corresponding to stochastic webs with square or hexagonal symmetry, respectively. (c) $\hbar/(2\pi)$ is integer for $l = 4$ while $\sqrt{3}\hbar/(4\pi)$ is integer for $l = 6$. When all these conditions hold, it follows from the results in Ref. [15] that $\hat{U}_T^l(x_c) = -1$ for $x_c = \pi/2$, $3\pi/2$ and $l = 4$, 6. In this paper, only the case of $l = 4$ with $j/l = \frac{1}{4}$ ($\alpha = \pi/2$) will be considered. Using general results [15], one finds that the evolution operator $\hat{U}_T^4(x_c)$ in this case is equal to $-\hat{U}(x_c)$, where

$$\hat{U}(x_c) = \exp[i\mu\cos(x_c - \hat{u})]\exp[i\mu\cos(x_c + \hat{v})]$$
$$\times \exp[i\mu\cos(x_c + \hat{u})]\exp[i\mu\cos(x_c - \hat{v})] \quad (3)$$

and $\mu = K/\hbar$. We show in the Appendix (Sec. A 1) that the range of x_c in Eq. (3) can be restricted to $[0, \pi/2]$ without loss of generality. Thus, only the QAR point $x_c = \pi/2$ will be considered; $\hat{U}(\pi/2) = 1$ for integer $\hbar/(2\pi)$.

We now extend the notion of HB [6] to the operator (3). Let us denote by E and Ψ, respectively, the quasienergies (QEs) and QE eigenstates, defined by $\hat{U}(x_c)\Psi = \exp(-i\mu E)\Psi$, with E lying in the interval $[-\pi/\mu, \pi/\mu]$. We then define the HB as the plot of the QE spectrum $E(\hbar)$ as a function of $\hbar$, for $0 \le \hbar \le 2\pi$, at *fixed* μ. Such a plot was introduced in Ref. [13] for the KHM and is motivated by the fact, shown in the Appendix (Sec. A 2), that $E(\hbar)$ is 2π-periodic in $\hbar$ at fixed μ. A small value of μ characterizes a HB associated with a "semiclassical weak-chaos regime," i.e., a regime of small $K = \hbar\mu$ for all small values of $\hbar$, $\hbar < 1$. We also show in the Appendix (Sec. A 2) that: (a) For rational $\hbar/(2\pi) = q/p$ (q and p are coprime integers), the QE spectrum consists of p bands, each q-fold degenerate. (b) The HB has reflection symmetry around $\hbar = \pi$ [i.e., $E(2\pi - \hbar) = E(\hbar)$] only if $x_c = 0$ or $x_c = \pi/2$. Examples of HBs, plotted for all $\hbar = 2\pi q/p$ with $1 \le q \le p \le 50$, are shown in Fig. 2 for three values of x_c. We see that for $x_c = \pi/2$ [Fig. 2(c)] the QE spectrum $E \to 0$ as $\hbar \to 2\pi$ or $\hbar \to 0$, reflecting the QAR phenomenon, $\hat{U}(\pi/2) = 1$ for $\hbar = 2\pi$.

The unitary operator (3) can be formally written as $\hat{U}(x_c) = \exp[-i\mu\hat{H}_{\text{eff}}(x_c)]$, where $\hat{H}_{\text{eff}}(x_c)$ is an effective Hamiltonian for the problem. Clearly, if E' is the "energy" spectrum of $\hat{H}_{\text{eff}}(x_c)$, the QE spectrum E is just E' modulo the interval $[-\pi/\mu, \pi/\mu]$. Thus, the "unfolded" HB is the spectrum E' plotted as a function of $\hbar$ ($0 \le \hbar \le 2\pi$) at fixed μ. The dependence of some general HB features on x_c can be understood on the basis of an expression for $\hat{H}_{\text{eff}}(x_c)$ which we now derive. We first note that the arguments of the exponents in Eq. (3) involve simple operators $\exp(\pm i\hat{u})$ and
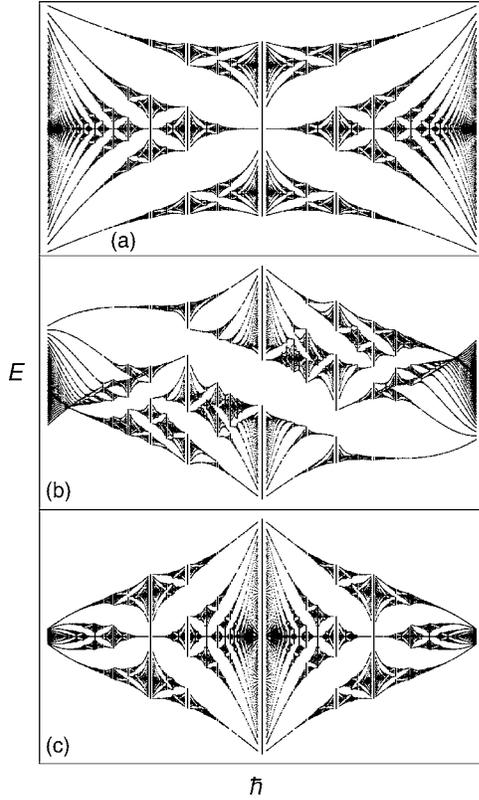
FIG. 2. HBs $E(\hbar)$ for $\mu=0.5$ and (a) $x_{\rm c}=0$, $-4\leqslant E\leqslant 4$; (b) $x_{\rm c}=1.47$, $-1\leqslant E\leqslant 1$; (c) $x_{\rm c}=\pi/2$, $-1\leqslant E\leqslant 1$.

$\exp(\pm i\hat{v})$, giving just translations by $\pm\hbar$ in the (u,v) phase plane. Using then the known formula [26]

$$\exp(A)\exp(B) = \exp\left(A + B + \frac{1}{2}[A,B] + \frac{1}{12}[A,[A,B]]\right.$$
$$\left. + \frac{1}{12}[[A,B],B] + \cdots\right), \qquad (4)$$

valid for arbitrary operators A and B, one can verify by tedious but straightforward algebra that $\hat{H}_{\rm eff}(x_{\rm c})$ can be expressed as a power expansion in a parameter ϵ,

$$\hat{H}_{\rm eff}(x_{\rm c}) = \sum_{r=0}^{\infty} \epsilon^r \hat{H}_r(x_{\rm c}), \quad \epsilon = \mu\sin(\hbar/2) = \frac{K}{2}\frac{\sin(\hbar/2)}{\hbar/2}.$$
$$(5)$$

The zero-order coefficient in Eq. (5) is

$$\hat{H}_0(x_{\rm c}) = -2\cos(x_{\rm c})[\cos(\hat{u}) + \cos(\hat{v})]. \qquad (6)$$

The operator (6) is a Harper Hamiltonian and if ϵ is sufficiently small, $2|\cos(x_{\rm c})/\epsilon| \gg 1$, is the dominant term in the expansion (5) for most values of $x_{\rm c}$. For general μ, ϵ is small provided $\hbar/(2\pi)$ is sufficiently close to an integer. In a weak-chaos (small μ or K) regime, on which we shall focus, ϵ is globally small for *all* $\hbar$. Then, for $2|\cos(x_{\rm c})/\epsilon| \gg 1$, the HB is essentially the standard one for the Harper model [6], see Fig. 2(a). For $2|\cos(x_{\rm c})/\epsilon| \lesssim 1$, higher-order coefficients in Eq. (5) become significant, especially for $\hbar \approx \pi$ (largest ϵ
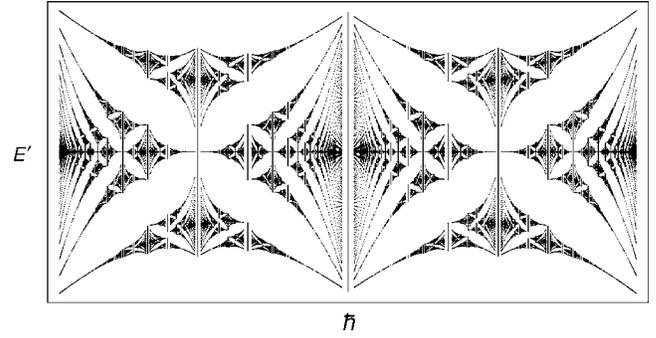

FIG. 3. Perturbed double HB $E'(\hbar)$ $(-2\leqslant E'\leqslant 2)$, obtained by locally scaling the HB in Fig. 2(c) by $\epsilon^{-1}=[\mu\sin(\hbar/2)]^{-1}$. The perturbation is reflected by the fact that the spectral width $\Delta E'(\pi)$ (at the HB center) is slightly smaller than the maximal width $\Delta E'(2\pi)=4$.

at fixed μ), leading to a clearly nonstandard HB with a visible reflection-symmetry breaking; see Fig. 2(b).

For $x_{\rm c}=\pi/2$, $\hat{H}_0$ *vanishes*. If also $\hbar/(2\pi)$ is integer, $\epsilon=0$ and thus $\hat{H}_{\rm eff}=0$, implying $\hat{U}(\pi/2)=1$ (QAR). Small values of ϵ for $x_{\rm c}=\pi/2$ define a *QAR vicinity*; thus, a weak-chaos regime at $x_{\rm c}=\pi/2$ corresponds to a QAR vicinity for arbitrary $\hbar$. Now, $\hat{H}_{\rm eff}(\pi/2)=\epsilon\hat{H}_1+\epsilon^2\hat{H}_2+\cdots$, and we find that

$$\hat{H}_1(\pi/2) = -[\cos(\hat{u}+\hat{v}) + \cos(\hat{u}-\hat{v})]. \qquad (7)$$

Since the operators $\hat{u}'=\hat{u}+\hat{v}$ and $\hat{v}'=\hat{v}-\hat{u}$ are clearly conjugate, $[\hat{u}',\hat{v}']=i\hbar'$ with $\hbar'=2\hbar$, we see that $\hat{H}_1$ in Eq. (7) is again a Harper Hamiltonian. When $\hbar$ varies from 0 to 2π, $\hbar'=2\hbar$ varies from 0 to 4π. Then, the HB for $\hat{H}_{\rm eff}/\epsilon=\hat{H}_1+\epsilon\hat{H}_2+\cdots$ is a perturbed doubled version of the standard HB, see Fig. 3. A simple measure of the perturbation of this HB is $P=|1-\Delta E'(\pi)/\Delta E'(2\pi)|$, where $\Delta E'(\hbar)$ is the width of the spectrum of $\hat{H}_{\rm eff}/\epsilon$. The exact result $P=1-\mu^{-2}\arcsin[\sin^2(\mu)]=\mu^2/3+\cdots$ is easily derived (see note [27]). As $\hbar$ approaches its QAR value of 2π (or 0 at fixed μ), the width $\Delta E(\hbar)\approx\mu\sin(\hbar/2)\Delta E'(2\pi)$ of the QE spectrum vanishes almost linearly in $\hbar$, see Fig. 2(c).

A simple consequence of the approximately doubled structure of the HB for $\hat{H}_{\rm eff}(\pi/2)/\epsilon$ is that if $\hbar=2\pi q/p$ and p is *even*, $p=2p'$, the p bands in this HB actually form p' pairs of overlapping bands. This is because the spectrum of the Harper Hamiltonian (7) for $\hbar'=2\hbar=2\pi q/p'$ always consists of p' nonoverlapping bands [6]. Each such band must then correspond to a pair of overlapping bands of $\hat{H}_{\rm eff}$ for sufficiently small ϵ. Thus, the number of gaps in the spectrum for even p is more than halved when $x_{\rm c}$ is varied from 0 to $\pi/2$.

III. CLASSICAL LIMITS AND ANALOGS

In this section, we consider classical limits and analogs of some of the results above. The classical one-period map for the system (2) in the case of $\alpha=\pi/2$ is [22]

$$M: u_{s+1} = v_s, \quad v_{s+1} = -u_s + K\sin(x_c - v_s). \quad (8)$$

The fourth iterate M^4 of M is the classical map corresponding to the evolution operator $\hat{U}(x_c)$ in Eq. (3). One can easily show that M^4 is a near-identity map for small K [23], i.e., $u_{t+1} = u_t + O(K)$, $v_{t+1} = v_t + O(K)$, where t denotes now an integer time index counting iterations of M^4. It is then clear from the expression $\hat{U}(x_c) = \exp[-iK\hat{H}_{\text{eff}}(x_c)/\hbar]$ that the classical limit ($\hbar \to 0$, $\epsilon \to K/2$) of $\hat{H}_{\text{eff}}(x_c)$ is an integrable Hamiltonian $H_{\text{eff}}(u,v;x_c)$ generating, in a continuous time denoted here by t', a phase-space flow which approximates the near-integrable map M^4 at times $t' = Kt$:

$$\frac{\partial H_{\text{eff}}}{\partial v} = \frac{du}{dt'} \approx \frac{u_{t+1} - u_t}{K}, \quad -\frac{\partial H_{\text{eff}}}{\partial u} = \frac{dv}{dt'} \approx \frac{v_{t+1} - v_t}{K}. \quad (9)$$

Expressions for $KH_{\text{eff}}/4$ as power expansions in K are given in Ref. [23]. Like $\hat{U}(x_c)$, M^4 and $H_{\text{eff}}(u,v;x_c)$ are generally periodic in the phase space (u,v) with a unit cell of area $4\pi^2$, so that the orbit structure of M^4 or the flow (9) feature the same periodicity, as is clearly shown in Figs. 1(a) and 1(b). For $x_c = \pi/2$, however, the dominant term in $H_{\text{eff}}(u,v;\pi/2)$ is the classical analog H_1 of (7), which is periodic with a unit cell of area $2\pi^2$, *half* the size of the usual unit cell; this periodicity is then approximately exhibited by the corresponding orbit structure, compare Fig. 1(c) with Fig. 1(a). This is the classical fingerprint in the approximate doubling of the HB for $x_c = \pi/2$ (see previous section and Fig. 3).

The hyperbolic fixed points of M^4 form a periodic array connected by the stochastic web, see Fig. 1. As shown in Ref. [23], the width of the web for small K is proportional to $\exp[-\pi^2/\ln(\lambda)]$, where λ is the largest eigenvalue of the linearization of M^4 at a hyperbolic fixed point and is given by $\lambda \approx 1 + 2K\cos(x_c)$ for $\cos(x_c) \gg K/4$ and by $\lambda \approx 1 + K^2$ for $x_c = \pi/2$. Thus, the latter case is characterized by a significantly small web width and slow chaotic diffusion relative to those for most values of x_c [23]. These features may be viewed as classical analogs of the QAR phenomenon, including some quantum behaviors in a QAR vicinity (see Sec. IV C and Sec. V).

IV. QUANTUM DIFFUSION FOR GENERAL x_c

In this section, we study the quantum diffusion exhibited by wave packets evolving under the operator (3) and its effective-Hamiltonian approximations.

A. General quantum evolution and periodic wave packets

A general wave packet $|\Phi\rangle$ for the original 2D problem (1) can be naturally expressed in a representation based on the two degrees of freedom (conjugate pairs) $(\hat{u},\hat{v})$ and $(\hat{x}_c,\hat{y}_c)$, for example, in the (u,x_c) representation, $\langle u,x_c|\Phi\rangle = \Phi(u,x_c)$. The time evolution of $\Phi(u,x_c)$ can be decomposed into the independent evolutions for the separate, conserved x_c values,

$$\Phi(u,x_c;t) = \hat{U}^t(x_c)\Phi(u,x_c), \quad (10)$$

t being the integer time index. We show in the Appendix (Sec. A 3) that the quantum dynamics (10) can be fully reproduced from that of wave packets on a cylindrical phase space, $0 \le u < 2\pi$, $-\infty < v < \infty$, with $\Phi(u,x_c)$ 2π-periodic in u:

$$\Phi(u,x_c) = \sum_{n=-\infty}^{\infty} \varphi(n,x_c)\exp(inu). \quad (11)$$

Here the Fourier coefficients $\varphi(n,x_c)$ give the (v,x_c) representation of $|\Phi\rangle$ on the cylinder, with v quantized in units of $\hbar$, $v = n\hbar$. The quantum evolution of the wave packet (11) in the (n,x_c) representation,

$$\varphi(n,x_c;t) = \hat{U}^t(x_c)\varphi(n,x_c), \quad (12)$$

can be easily calculated as in the kicked-rotor case [3], by using a fast Fourier transform to switch from the position (u) to the momentum ($v = n\hbar$) representation (and vice versa) before the application of each factor in Eq. (3). The spreading of the wave packet (12) along the cylinder at fixed x_c is measured by the expectation value $\langle \hat{v}^2 \rangle_t$ of $\hat{v}^2$ in $\varphi(n,x_c;t)$:

$$\langle \hat{v}^2 \rangle_t = \frac{\hbar^2}{N(x_c)}\sum_{n=-\infty}^{\infty} n^2|\varphi(n,x_c;t)|^2, \quad N(x_c) = \sum_{n=-\infty}^{\infty} |\varphi(n,x_c)|^2. \quad (13)$$

The expectation value of $\hat{v}^2$ in the original *2D wave packet* $\varphi(n,x_c;t)$ (both n and x_c are variables) is given by

$$\overline{\langle \hat{v}^2 \rangle_t} = \hbar^2 \sum_{n=-\infty}^{\infty} n^2 \int |\varphi(n,x_c;t)|^2 dx_c, \quad (14)$$

where normalization of φ over (n,x_c) is assumed, $\int N(x_c)dx_c = 1$. We also show in the Appendix (Sec. A 3) that our main results below concerning $\langle \hat{v}^2 \rangle_t$ can be extended to the expectation value $\langle \omega^2(\hat{u}^2 + \hat{v}^2)/2 \rangle_t$ of the kinetic energy in an arbitrary wave packet (10). Thus, for convenience and without loss of generality, we shall restrict our attention to periodic wave packets (11) and to the expectation values (13) and (14).

B. Quantum diffusion at fixed x_c and global quantum diffusion

We have seen in Sec. II that if ϵ is sufficiently small, the dominant term in the expansion (5) of $\hat{H}_{\text{eff}}(x_c)$ for most values of x_c, including $x_c = \pi/2$, is a Harper Hamiltonian. It is known [8,9] that for irrational $\hbar/(2\pi)$ the latter Hamiltonian exhibits a fractal spectrum and, asymptotically in time, an approximate quantum diffusion of the second moment of a wave packet. Therefore, we can expect a similar behavior of $\langle \hat{v}^2 \rangle_t$ under $\hat{U}(x_c) = \exp[-i\mu\hat{H}_{\text{eff}}(x_c)]$ for irrational $\hbar/(2\pi)$ and sufficiently large t: $\langle \hat{v}^2 \rangle_t \approx 2D(x_c)t$, where $D(x_c)$ is the diffusion coefficient at fixed x_c.

As an illustration, let us choose the initial wave packet (11) as a periodized coherent state centered on some x_c-dependent point $(\bar{u},\bar{v})$,
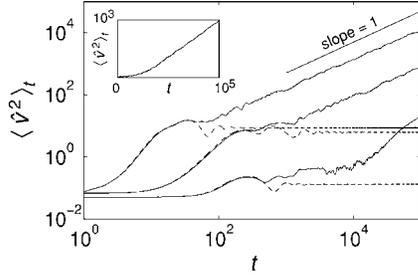
FIG. 4. Solid lines: $\langle \hat{v}^2 \rangle_t$ for $\hbar/(2\pi)=[51+(\sqrt{5}-1)/2]^{-1}$, $K=0.157$, and $x_c=0$ (upper line), $x_c=1.47$ (middle line), $x_c=\pi/2$ (lower line). Dashed lines: corresponding classical quantity $\langle v_t^2 \rangle$ for the same values of x_c (see text for more details). For the sake of visibility, the lines for $x_c=\pi/2$ were shifted below by multiplying both $\langle \hat{v}^2 \rangle_t$ and $\langle v_t^2 \rangle$ by 0.019 75. The inset shows the normal plot of $\langle \hat{v}^2 \rangle_t$ for $x_c=\pi/2$. The values of $\hbar$ and K above were used also to obtain the results in Figs. 5 and 6.

$$\Phi(u,x_c) = (\pi\hbar)^{-1/4} \sum_{m=-\infty}^{\infty} \exp\left\{ i \frac{\bar{v}(x_c)(u - 2\pi m)}{\hbar} \right.$$
$$\left. - \frac{[u - 2\pi m - \bar{u}(x_c)]^2}{2\hbar} \right\}. \quad (15)$$

For sufficiently small $\hbar$, a classical quantity analogous to the expectation value $\langle \hat{v}^2 \rangle_t$ in the wave packet (15) is the average $\langle v_t^2 \rangle$ of v_t^2 over an ensemble of initial conditions (u_0,v_0) uniformly distributed in a disk centered on $(\bar{u},\bar{v})$ and of radius $\sqrt{2\hbar}$; (u_t,v_t) is the tth iterate of (u_0,v_0) under the map M^4 (see Sec. III). Figure 4 shows log-log plots of $\langle \hat{v}^2 \rangle_t$ and $\langle v_t^2 \rangle$ for $\hbar/(2\pi)=[51+(\sqrt{5}-1)/2]^{-1}$, $K=0.157$, and $0 < t \leq 10^5$ in the three cases of x_c considered in Figs. 1 and 2; in each case, $(\bar{u},\bar{v})$ was chosen as a hyperbolic fixed point of the corresponding map M^4. We see that $\langle \hat{v}^2 \rangle_t$ and $\langle v_t^2 \rangle$ essentially coincide up to some time $t=t^*(x_c)$, after which $\langle v_t^2 \rangle$ stops spreading and there occurs a crossover of $\langle \hat{v}^2 \rangle_t$ to an approximate quantum diffusion, $\langle \hat{v}^2 \rangle_t \approx 2D(x_c)t$. In the case of $x_c=\pi/2$, this diffusion is shown more clearly by the normal plot of $\langle \hat{v}^2 \rangle_t$ in the inset of Fig. 4.

These results can be understood as follows. The irrational value of $\hbar/(2\pi)$ chosen above represents a semiclassical regime in which $h=2\pi\hbar$ is small relative to the area $4\pi^2$ of a unit cell but large relative to the width $\sim\exp[-\pi^2/\ln(\lambda)]$ of the stochastic web for $K=0.157$ (see classical details in Sec. III). Thus, classical chaos leaves almost no fingerprints in the quantum properties which should then resemble those of the integrable approximation of the system given by the effective Hamiltonian $H_{\mathrm{eff}}(x_c)$, with the stochastic web replaced by its separatrix "skeleton" [21,23]. A classical ensemble of width $\sim\sqrt{2\hbar}$ centered on a hyperbolic fixed point will lie mostly in the stable regions within the unit cells and will spread to its maximal extent (of the order of the size of one unit cell) in a time $t=t^*(x_c)$ roughly proportional to $\ln(1/\hbar)/\ln[\lambda(x_c)]$; this agrees with numerical estimates of $t^*(x_c)$ in all cases considered, including those shown in Fig. 4. The quantum wave packet, however, will continue to spread due to tunneling

between neighboring unit cells, leading to quantum diffusion [8,9].

Assuming the asymptotic quantum-diffusion behavior of $\langle \hat{v}^2 \rangle_t$, $\langle \hat{v}^2 \rangle_t \approx 2D(x_c)t$, to hold approximately for all x_c, one finds from Eqs. (13) and (14) that the 2D wave packet (12) can be characterized by a more realistic quantity, its global diffusion coefficient $\bar{D}$, given by a weighted average of $D(x_c)$ over x_c:

$$\overline{\langle \hat{v}^2 \rangle_t} \approx 2\bar{D}t, \quad \bar{D} = \int N(x_c)D(x_c)dx_c, \quad (16)$$

where $N(x_c)$ is defined in Eq. (13). The global diffusion (16) will be briefly considered at the end of this section.

C. x_c dependence of the quantum-diffusion coefficient for simple wave packets

We now consider the x_c dependence of the quantum-diffusion coefficient D. It is clear from Eq. (12) that this dependence is generally due to that of both $\hat{U}(x_c)$ and the initial wave packet $\varphi(n,x_c)$. For simplicity, we shall restrict ourselves from now on to the class of wave packets for which one has a separation of the (n,x_c) variables, $\varphi(n,x_c) = \chi(x_c)\psi(n)$ [$\chi(x_c)$ and $\psi(n)$ are assumed to be normalized]. Then, $\varphi(n,x_c;t)=\chi(x_c)\hat{U}^t(x_c)\psi(n)$, so that $\langle \hat{v}^2 \rangle_t$ in Eq. (13) is independent of $\chi(x_c)$ and the x_c dependence of $\langle \hat{v}^2 \rangle_t$ for fixed $\psi(n)$ is completely due to that of $\hat{U}(x_c)$. This allows one to derive an approximate formula for $D(x_c)$ in the case of $2|\cos(x_c)/\epsilon| \gg 1$. In this case, which covers most values of x_c, the effective Hamiltonian $\hat{H}_{\mathrm{eff}} \approx \hat{H}_0$, where $\hat{H}_0$ is given by Eq. (6). The tth power of the approximate evolution operator $\hat{U}_0=\exp(-i\mu\hat{H}_0)$ can be written as follows:

$$\hat{U}_0^t(x_c) = \exp\{2iK\cos(x_c)t[\cos(\hat{u}) + \cos(\hat{v})]/\hbar\}. \quad (17)$$

Relation (17) implies that the wave packet $\psi(n,x_c;t) = \hat{U}_0^t(x_c)\psi(n)$ depends on K, x_c, and t only through the combination $K\cos(x_c)t$. Thus, if one assumes an asymptotic quantum-diffusive behavior, $\langle \hat{v}^2 \rangle_t \approx 2D(x_c)t$, accurately described by $\hat{U}_0$, $D(x_c)$ must be approximately linear in $K\cos(x_c)$:

$$D(x_c) \approx 2D_{\mathrm{H}}^{(\pm)}K\cos(x_c), \quad 2|\cos(x_c)/\epsilon| \gg 1. \quad (18)$$

Here the proportionality constants $D_{\mathrm{H}}^{(+)}$ and $D_{\mathrm{H}}^{(-)}$ are associated with the x_c intervals where $\cos(x_c)>0$ and $\cos(x_c)<0$, respectively; assuming that $K>0$ for definiteness, one has $D_{\mathrm{H}}^{(+)}>0$ and $D_{\mathrm{H}}^{(-)}<0$ since $D(x_c)>0$. The constants $D_{\mathrm{H}}^{(+)}$ and $|D_{\mathrm{H}}^{(-)}|$ are just the diffusion coefficients for $\langle \hat{v}^2 \rangle_t$ under the standard Harper evolution operator $\hat{U}_{\mathrm{H}}=\exp\{i[\cos(\hat{u}) + \cos(\hat{v})]/\hbar\}$ and its inverse $\hat{U}_{\mathrm{H}}^{-1}$, respectively. For general $\psi(n)$, $D_{\mathrm{H}}^{(+)} \neq |D_{\mathrm{H}}^{(-)}|$. However, if $\psi(n)$ satisfies some symmetry properties, e.g., its u representation is given by the right-hand side of Eq. (15) with $\bar{u}$ a multiple of π (as in the example below), one can show that $D_{\mathrm{H}}^{(+)}=|D_{\mathrm{H}}^{(-)}|$ (see Appendix, Sec. A 4). Formula (18) can then be rewritten as $D(x_c)$
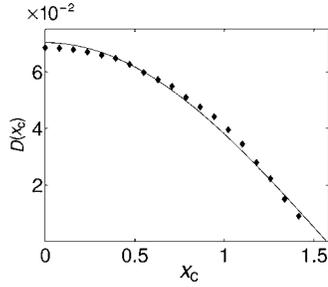
FIG. 5. Diamonds: numerical results for the quantum-diffusion coefficient $D(x_c)$ (see text for more details). Solid line: least-square fit of formula (18) to the numerical data, $D_H^{(+)} = 0.224$.

$\approx 2D_H K |\cos(x_c)|$ with the same constant D_H for all x_c satisfying $2|\cos(x_c)/\epsilon| \gg 1$.

As a check of formula (18), we have calculated $D(x_c)$ for $\hbar/(2\pi) = [51 + (\sqrt{5}-1)/2]^{-1}$, $K = 0.157$, and $x_c = k\pi/40$, $k = 0, 1, \ldots, 18$ by a linear fit to $\langle \hat{v}^2 \rangle_t$ ($0 < t \leq 10^4$), evolving under the exact operator $\hat{U}(x_c)$. The u representation of the initial wave packet $\psi(n)$ is given by the right-hand side of Eq. (15) with $(\bar{u}, \bar{v}) = (\pi, 0)$, a hyperbolic fixed point for $x_c = 0$ [see Fig. 1(a)]. The results, shown in Fig. 5, agree satisfactorily with a least-square fit of the function (18) to the data.

Consider now the case of $x_c = \pi/2$. From the fact that $\hat{H}_{\text{eff}}(\pi/2) \approx \epsilon \hat{H}_1(\pi/2) = O(K)$, one expects, using arguments similar to those leading to formula (18), that $D(\pi/2)$ should be approximately quadratic in K. In Table I, we present results concerning the K dependence of $D(0)/K$ and $D(\pi/2)/K^2$. The values of $D(0)$ and $D(\pi/2)$ were calculated by a linear fit to $\langle \hat{v}^2 \rangle_t$ ($0 < t \leq 10^4$ for $x_c = 0$ and $0 < t \leq 10^5$ for $x_c = \pi/2$), evolving under the exact operator (3); for both $x_c = 0$ and $x_c = \pi/2$, the initial wave packet is given by the right-hand side of Eq. (15) with $(\bar{u}, \bar{v})$ chosen as a hyperbolic fixed point of the corresponding map M^4. The results for $D(0)/K$ agree very well with the approximate linearity in K predicted by formula (18). On the other hand, $D(\pi/2)$ appears to decrease faster than K^2 as K decreases, which may indicate that high-order corrections to $\hat{H}_{\text{eff}}$ for $x_c = \pi/2$ have a stronger impact than for $x_c = 0$. In any case, Table I provides evidence that as K decreases $D(\pi/2)$ becomes significantly smaller than typical values of $D(x_c)$.

We end this section by a brief consideration of the global quantum diffusion (16) in the case of the initial wave packets $\varphi(n, x_c) = \chi(x_c)\psi(n)$. For such a wave packet, formula (18) can be used to calculate approximately the global diffusion coefficient $\bar{D}$, with $N(x_c) = |\chi(x_c)|^2$ in Eqs. (13) and (16). Choosing $N(x_c)$ uniform, $N(x_c) = 2/\pi$, for $0 \leq x_c < \pi/2$ and vanishing outside this interval, one finds from Eqs. (16) and

TABLE I. $D(0)/K$ and $D(\pi/2)/K^2$ for several values of K.

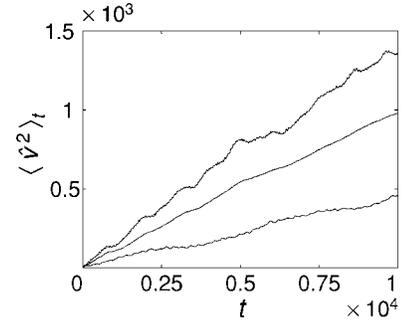| K	0.15	0.157	0.17	0.18	0.19	0.2
$D(0)/K$	0.458	0.459	0.461	0.461	0.460	0.459
$D(\pi/2)/K^2$	0.219	0.226	0.237	0.243	0.244	0.243

FIG. 6. Middle line: global quantum diffusion of $\overline{\langle \hat{v}^2 \rangle_t}$, given by a uniform average of $\langle \hat{v}^2 \rangle_t$ over $x_c = k\pi/40$, $k = 0, 1, \ldots, 18$ (see text for more details). The upper and lower lines correspond to $\langle \hat{v}^2 \rangle_t$ for $x_c = 0$ ($k = 0$) and $x_c = 2\pi/5$ ($k = 16$), respectively.

(18) that $\bar{D} \approx 4D_H^{(+)} K/\pi$. Much smaller values of $\bar{D}$ are obtained if $N(x_c)$ is strongly localized around $x_c = \pi/2$. Figure 6 shows the time evolution of $\overline{\langle \hat{v}^2 \rangle_t}$, given by a uniform average of $\langle \hat{v}^2 \rangle_t$ over $x_c = k\pi/40$, $k = 0, 1, \ldots, 18$, where $\langle \hat{v}^2 \rangle_t$ for each of these x_c values was calculated as specified above for obtaining the results in Fig. 5. We also show in Fig. 6 the functions $\langle \hat{v}^2 \rangle_t$ for $x_c = 0$ ($k = 0$) and $x_c = 2\pi/5$ ($k = 16$). As expected, averaging over x_c removes from $\overline{\langle \hat{v}^2 \rangle_t}$ much of the fluctuations exhibited by $\langle \hat{v}^2 \rangle_t$ at fixed x_c.

V. SUMMARY AND CONCLUSIONS

Our study of the quantized system (2) for general x_c has revealed the significant impact of the transition $x_c \to \pi/2$ to a QAR vicinity on the spectral and quantum-diffusion properties in a weak-chaos (small K) regime. In this transition, the dominant term in the effective-Hamiltonian expansion (5) changes from $\hat{H}_0$ to $\epsilon \hat{H}_1$ in a x_c window of width $\sim \epsilon$ around $x_c = \pi/2$, where $\hat{H}_0$ vanishes. Both $\hat{H}_0(x_c)$ and $\hat{H}_1(\pi/2)$ are Harper Hamiltonians, but $\hat{H}_1(\pi/2)$ is periodic in phase space with a unit cell half the size of that of $\hat{H}_0(x_c)$. As a consequence, the HB for $x_c = \pi/2$ is essentially a perturbed doubled version of the standard HB for the Harper model (see Fig. 3). Thus, as x_c is varied from 0 to $\pi/2$, there must occur strong changes in the HB structure and the spectral properties (see Fig. 2 and the end of Sec. II), reflecting corresponding changes in the classical web structure due to bifurcations [23] (see Fig. 1). A more detailed investigation of the fingerprints of these bifurcations in the quantum properties is planned for a future work.

The quantum diffusion of wave packets for the system (2) was characterized by a coefficient $D(x_c)$ at fixed x_c and by a global coefficient $\bar{D}$. Formula (18) for $D(x_c)$ was derived on the basis of the approximate effective Hamiltonian $\hat{H}_0(x_c)$ and it agrees reasonably well with numerical results for sufficiently small K (see Fig. 5 and Table I). This formula and numerical evidence indicate that $D(x_c)$ is strongly reduced as $x_c \to \pi/2$: $D(\pi/2)$ appears to be not larger than $O(\epsilon)$ relative to typical values of $D(x_c)$. This phenomenon is of a purely quantum nature but it is analogous to the relatively slow

classical chaotic diffusion for $x_c = \pi/2$ in a weak-chaos regime [23]. An interesting but apparently difficult problem is to obtain a refined formula for $D(x_c)$, extending the zero-order result (18) to the small x_c window around $x_c = \pi/2$ where higher-order terms in the expansion (5) must be taken into account.

The strong variation of $D(x_c)$ with x_c is exhibited in practice by the global quantum diffusion of a 2D wave packet for all x_c. If the potential $\cos(x)$ in Eq. (1) is replaced by $\cos(x - \theta)$, where θ is an adjustable phase, one can "filter" the wave-packet component associated with an arbitrary value of $x_c \approx \theta + \pi/2$ as the component having the smallest quantum-diffusion rate. The new quantum phenomena predicted by the realistic, general-x_c approach to (1) may be observed in possible experimental realizations of this system.

APPENDIX

1. Exact relation between system (2) and KHM and relevant x_c range

The evolution operator (3) for the system (2) in the case of $\alpha = \pi/2$ is equivalent to $\hat{U}'(x_c) = \exp[-i\mu W(\hat{v})]\hat{U}(x_c)\exp[i\mu W(\hat{v})]$, where $W(v) = -\cos(x_c - v)$. One has

$$\hat{U}'(x_c) = \hat{U}_{\text{KHM}}^{(+)}\hat{U}_{\text{KHM}}^{(-)}, \tag{A1}$$

where

$$\hat{U}_{\text{KHM}}^{(\pm)} = \exp[-i\mu W(\pm\hat{v})]\exp[-i\mu W(\pm\hat{u})]$$

is the one-period evolution operator for the generalized KHM [16,17] with Hamiltonian $H = W(\pm v) + W(\pm u)\sum_{s=-\infty}^{\infty}\delta(t/K - s)$. This reduces to the usual KHM Hamiltonian, with $W(v) = \cos(v)$ (up to a sign), only for $x_c = 0, \pi$. Then, $\hat{U}_{\text{KHM}}^{(+)} = \hat{U}_{\text{KHM}}^{(-)} = \hat{U}_{\text{KHM}}$ and the exact relation $\hat{U}'(x_c) = \hat{U}_{\text{KHM}}^2$ follows from Eq. (A1).

The evolution operator (3) satisfies also the similarity relations

$$\hat{U}(x_c + \pi) = \hat{D}\hat{U}(x_c)\hat{D}^{-1}, \quad \hat{U}(-x_c) = \hat{S}\hat{U}(x_c)\hat{S}^{-1}, \tag{A2}$$

where

$$\hat{D} = \exp(\pi i\hat{u}/\hbar)\exp(\pi i\hat{v}/\hbar),$$

$$\hat{S} = \exp[-i\mu\cos(x_c + \hat{v})]\exp[-i\mu\cos(x_c - \hat{u})].$$

Since $\hat{U}(x_c)$ is 2π-periodic in x_c, relations (A2) imply that the range of x_c can be restricted to $[0, \pi/2]$ without loss of generality.

2. Quasienergy band spectrum and some of its basic properties

Using relation (A1), the results in Ref. [17] concerning the quasienergy (QE) band spectra of generalized KHMs can be straightforwardly extended to the operator $\hat{U}'(x_c)$, which is equivalent to the evolution operator $\hat{U}(x_c)$ in Eq. (3) and thus has the same QE spectra as those of $\hat{U}(x_c)$. For $\hbar = 2\pi q/p$ (q and p are coprime integers), $\hat{U}'(x_c)$ and the phase-space translations $\hat{D}_1 = \exp(2\pi i\hat{u}/\hbar)$ and $\hat{D}_2 = \exp(ip\hat{v})$ form a complete set of commuting operators. Their simultaneous eigenstates are given, in the v representation, by

$$\Psi_{b,\mathbf{w},x_c}(v) = \sum_{m=0}^{p-1}\phi_b(m;\mathbf{w};x_c)\sum_{n=-\infty}^{\infty}\exp[in(w_1 + m\hbar)/q]$$

$$\times \delta(v - w_2 + 2\pi n/p).$$

Here the index $b = 1, \ldots, p$ labels p QE bands; $\mathbf{w} = (w_1, w_2)$ is a Bloch wave vector spanning a band and ranging in the "Brillouin zone" $0 \leq w_1 < \hbar$, $0 \leq w_2 < 2\pi/p$; and $\{\phi_b(m;\mathbf{w};x_c)\}_{m=0}^{p-1}$, $b = 1, \ldots, p$, are p independent vectors of coefficients. The corresponding eigenvalues of $\hat{U}'(x_c)$ are $\exp[-i\mu E_b(\mathbf{w};x_c)]$, where $E_b(\mathbf{w};x_c)$ is a QE band. It is easy to see that $\hat{U}'(x_c)$ commutes with $\hat{D}_0 = \exp(2\pi i\hat{v}/\hbar)$ and also that $\hat{D}_0^q = \hat{D}_2$. Then, the q states $\Psi_{b,\mathbf{w},x_c}^{(d)} = \hat{D}_0^d\Psi_{b,\mathbf{w},x_c}$, $d = 0, \ldots, q-1$, are different eigenstates of $\hat{U}'(x_c)$, all associated with the *same* eigenvalue. Therefore, each band is q-fold degenerate.

The p vectors $\{\exp(imw_2)\phi_b(m;\mathbf{w};x_c)\}_{m=0}^{p-1}$, $b = 1, \ldots, p$, are the eigenvectors of a $p \times p$ $\mathbf{w}$-dependent matrix $\mathbf{M}(\mathbf{w};x_c)$,

$$\mathbf{M}(\mathbf{w};x_c) = \mathbf{M}^{(+)}(\mathbf{w};x_c)\mathbf{M}^{(-)}(\mathbf{w};x_c), \tag{A3}$$

where $\mathbf{M}^{(\pm)}(\mathbf{w};x_c)$ are matrices corresponding to the operators $\hat{U}_{\text{KHM}}^{(\pm)}$ in relation (A1) and whose elements can be explicitly written using the results in Ref. [17]:

$$\mathbf{M}_{m,m'}^{(\pm)}(\mathbf{w};x_c) = \exp[i\mu\cos(x_c \mp w_1 \mp m'\hbar)]$$

$$\times \sum_{g=-\infty}^{\infty}J_{\mp(gp+m'-m)}(\mu,x_c)\exp(igpw_2),$$

$$\tag{A4}$$

where $m,m' = 0, \ldots, p-1$ and $J_m(\mu,x_c) = (2\pi)^{-1}\int_0^{2\pi}\exp[im(x_c - u) + i\mu\cos(u)]du$. It is clear from Eq. (A4) that the matrix (A3), and therefore the QE spectrum, is 2π-periodic in $\hbar$ at fixed μ. In addition, the matrix (A3) is invariant under the "reflection" $\hbar \to 2\pi - \hbar$ at fixed μ provided x_c and w_1 satisfy the two relations

$$x_c \mp w_1 = -x_c \pm w_1 + 2\pi j_\pm \tag{A5}$$

for some integers $j_\pm$. The solution of Eq. (A5) for x_c is $x_c = \pi(j_+ + j_-)/2$. Since x_c can be restricted to $[0, \pi/2]$ (see Sec. A 1), we see that the QE spectrum is invariant under $\hbar \to 2\pi - \hbar$ at fixed μ only if $x_c = 0, \pi/2$.

3. General quantum evolution in terms of periodic-wave-packet evolutions

Following Ref. [4], let us express the momentum v in the form $v = (n + \beta)\hbar$, where n and β are, respectively, the integer and fractional parts of $v/\hbar$. The (v, x_c) representation of a general 2D wave packet $|\Phi\rangle$ for the system (1) will be then denoted by $\varphi(n + \beta, x_c)$. From the relation between the (u, x_c) and the (v, x_c) representations, one finds that

$$\Phi(u, x_c) = \frac{1}{\hbar} \int \varphi(v/\hbar, x_c) \exp(iuv/\hbar) dv$$

$$= \int_0^1 d\beta \exp(i\beta u) \Phi_\beta(u, x_c), \qquad (A6)$$

where $\Phi(u, x_c)$ is the (u, x_c) representation of $|\Phi\rangle$ and

$$\Phi_\beta(u, x_c) = \sum_{n=-\infty}^{\infty} \varphi(n + \beta, x_c) \exp(inu). \qquad (A7)$$

Clearly, $\Phi_\beta(u, x_c)$ is 2π-periodic in u, so that relation (A6) provides the decomposition of $\Phi(u, x_c)$ into Bloch functions $\exp(i\beta u)\Phi_\beta(u, x_c)$ with quasimomentum β. Now, since the evolution operator $\hat{U}(\hat{u}, \hat{v}; x_c)$ in Eq. (3) is 2π-periodic in both $\hat{u}$ and $\hat{v}$, its application to such a Bloch function must "conserve" β; in fact, it is easy to see that

$$\hat{U}(\hat{u}, \hat{v}; x_c)[\exp(i\beta u)\Phi_\beta(u, x_c)] = \exp(i\beta u)\Phi_\beta'(u, x_c), \qquad (A8)$$

where

$$\Phi_\beta'(u, x_c) = \hat{U}\left(\hat{u} = u, \hat{v} = \hbar\beta - i\hbar\frac{d}{du}; x_c\right)\Phi_\beta(u, x_c). \qquad (A9)$$

The right-hand side of Eq. (A8) is also a Bloch function with quasimomentum β, since $\Phi_\beta'(u, x_c)$ is 2π-periodic in u due to Eq. (A9). Relation (A6) then implies that the evolution of a general wave packet $\Phi(u, x_c)$ under $\hat{U}(x_c)$ can be decomposed or "fibrated" [4] into independent evolutions at fixed β,

$$\hat{U}(x_c)\Phi(u, x_c) = \int_0^1 d\beta \exp(i\beta u)\hat{U}_\beta(x_c)\Phi_\beta(u, x_c), \qquad (A10)$$

where $\hat{U}_\beta(x_c)$ is the operator appearing on the right-hand side of Eq. (A9). Relation (A10) shows that the quantum dynamics (10) can be fully reproduced from that of periodic wave packets (A7) under the corresponding operators $\hat{U}_\beta(x_c)$.

We denote by $\varphi(v/\hbar, x_c; t) = \hat{U}^t(x_c)\varphi(v/\hbar, x_c)$ the wave packet at time t in the (v, x_c) representation and restrict our attention, as in Sec. IV C, to the case in which one has a separation of the (v, x_c) variables, $\varphi(v/\hbar, x_c) = \chi(x_c)\psi(v/\hbar)$, with normalized χ and ψ. The expectation value $\langle \hat{v}^2 \rangle_t$ of $\hat{v}^2$ in $\varphi(v/\hbar, x_c; t)$ can then be expressed as follows:

$$\langle \hat{v}^2 \rangle_t = \int v^2 |\psi(v/\hbar, x_c; t)|^2 dv = \int_0^1 d\beta N_\beta \langle \hat{v}^2 \rangle_{\beta, t}, \qquad (A11)$$

where $\psi(v/\hbar, x_c; t) = \hat{U}^t(x_c)\psi(v/\hbar)$,

$$\langle \hat{v}^2 \rangle_{\beta, t} = \frac{\hbar^2}{N_\beta} \sum_{n=-\infty}^{\infty} (n + \beta)^2 |\psi(n + \beta, x_c; t)|^2,$$

$$N_\beta = \sum_{n=-\infty}^{\infty} |\psi(n + \beta)|^2, \qquad (A12)$$

and $\psi(n + \beta, x_c; t) = \hat{U}_\beta^t(x_c)\psi(n + \beta)$. We notice that the expressions (A11) and (A12) are independent of $\chi(x_c)$ and their x_c dependence is completely due to that of $\hat{U}(x_c)$ or $\hat{U}_\beta(x_c)$. Fully analogous expressions can be written for the expectation values $\langle \hat{u}^2 \rangle_t$ and $\langle \hat{u}^2 \rangle_{\gamma, t}$, where γ is the quasimomentum characterizing Bloch functions 2π-quasiperiodic in the v direction. Let us now assume approximate quantum diffusions of $\langle \hat{v}^2 \rangle_{\beta, t}$ and $\langle \hat{u}^2 \rangle_{\gamma, t}$ for all (β, x_c), (γ, x_c), and for sufficiently large t, i.e., $\langle \hat{v}^2 \rangle_{\beta, t} \approx 2D_\beta(x_c)t$ and $\langle \hat{u}^2 \rangle_{\gamma, t} \approx 2D_{u,\gamma}(x_c)t$. The expectation value of the kinetic energy then exhibits the approximate diffusive behavior $\langle \omega^2(\hat{u}^2 + \hat{v}^2)/2 \rangle_t \approx 2D_{\mathrm{KE}}(x_c)t$, where

$$D_{\mathrm{KE}}(x_c) = (\omega^2/2)\left[\int_0^1 d\beta N_\beta D_\beta(x_c) + \int_0^1 d\gamma N_{u,\gamma} D_{u,\gamma}(x_c) \right].$$

Following the same reasoning as in the case of $\beta = 0$ considered in Sec. IV C, the diffusion coefficients $D_\beta(x_c)$, $D_{u,\gamma}(x_c)$, and $D_{\mathrm{KE}}(x_c)$ for sufficiently small K are expected to satisfy approximately formula (18) with $D_{\mathrm{H}}^{(\pm)}$ replaced by corresponding proportionality constants $D_{\mathrm{H},\beta}^{(\pm)}$, $D_{\mathrm{H},u,\gamma}^{(\pm)}$, and

$$D_{\mathrm{H,KE}}^{(\pm)} = (\omega^2/2)\left[\int_0^1 d\beta N_\beta D_{\mathrm{H},\beta}^{(\pm)} + \int_0^1 d\gamma N_{u,\gamma} D_{\mathrm{H},u,\gamma}^{(\pm)} \right].$$

4. Cases in which $D_{\mathrm{H},\beta}^{(+)} = |D_{\mathrm{H},\beta}^{(-)}|$

We show here that there are cases in which $D_{\mathrm{H},\beta}^{(+)} = |D_{\mathrm{H},\beta}^{(-)}|$ (similarly, one can show that there are cases in which $D_{\mathrm{H},u,\gamma}^{(+)} = |D_{\mathrm{H},u,\gamma}^{(-)}|$). The constants $D_{\mathrm{H},\beta}^{(+)}$ and $|D_{\mathrm{H},\beta}^{(-)}|$ are the diffusion coefficients for $\langle \hat{v}^2 \rangle_{\beta, t}$ under the standard Harper evolution operator $\hat{U}_{\mathrm{H}} = \exp\{i[\cos(\hat{u}) + \cos(\hat{v})]/\hbar\}$ and its inverse $\hat{U}_{\mathrm{H}}^{-1}$, respectively. In the u representation,

$$\hat{U}_{\mathrm{H}}^t(u) = \exp\left\{ \frac{it}{\hbar}\left[\cos(u) + \cos\left(i\hbar\frac{d}{du} \right) \right] \right\}. \qquad (A13)$$

Consider the Bloch state $\Lambda_\beta(u) = \exp(i\beta u)\Phi(u)$, where $\Phi(u)$ is given by the right-hand side of Eq. (15), and define the variable $u' = 2\bar{u} - u$. It is easy to see that

$$\Lambda_\beta(u) = C\Lambda_\beta^*(u'), \qquad (A14)$$

where $C = \exp[2i\bar{u}(\bar{v} + \beta)/\hbar]$ is a constant phase factor. Choosing now $\bar{u} = j\pi$, j integer, and using relations (A13) and (A14), we find that

$$\Lambda_\beta(u; -t) \equiv \hat{U}_H^{-t}(u)\Lambda_\beta(u) = C[\hat{U}_H^t(u')\Lambda_\beta(u')]^* = C\Lambda_\beta^*(u'; t).$$
$$(A15)$$

It follows from relation (A15) that

$$\langle\hat{v}^2\rangle_{\beta,-t} = -\hbar^2 \int_0^{2\pi} \Lambda_\beta^*(u; -t)\frac{d^2}{du^2}\Lambda_\beta(u; -t)du$$
$$= \langle\hat{v}^2\rangle_{\beta,t}^* = \langle\hat{v}^2\rangle_{\beta,t}, \qquad (A16)$$

since $\langle\hat{v}^2\rangle_{\beta,t}$ must be real (and positive). The equality $D_{H,\beta}^{(+)} = |D_{H,\beta}^{(-)}|$ is an immediate consequence of relation (A16).

[1] *Quantum Chaos, between Order and Disorder*, edited by G. Casati and B. Chirikov (Cambridge University Press, Cambridge, UK, 1995), and references therein.

[2] C. F. Bharucha, J. C. Robinson, F. L. Moore, B. Sundaram, Q. Niu, and M. G. Raizen, Phys. Rev. E **60**, 3881 (1999); B. Fischer, A. Rosen, and S. Fishman, Opt. Lett. **24**, 1463 (1999); A. Rosen *et al.*, J. Opt. Soc. Am. B **17**, 1579 (2000); S. Schlunk, M. B. d'Arcy, S. A. Gardiner, and G. S. Summy, Phys. Rev. Lett. **90**, 124102 (2003).

[3] D. R. Grempel, R. E. Prange, and S. Fishman, Phys. Rev. A **29**, 1639 (1984); D. L. Shepelyansky, Physica D **28**, 103 (1987).

[4] S. Fishman, I. Guarneri, and L. Rebuzzini, J. Stat. Phys. **110**, 911 (2003); S. Wimberger, I. Guarneri, and S. Fishman, Nonlinearity **16**, 1381 (2003).

[5] P. G. Harper, Proc. Phys. Soc., London, Sect. A **68**, 874 (1955).

[6] D. R. Hofstadter, Phys. Rev. B **14**, 2239 (1976).

[7] I. Dana and J. Zak, Phys. Rev. B **32**, 3612 (1985), and references therein.

[8] T. Geisel, R. Ketzmerick, and G. Petschel, Phys. Rev. Lett. **66**, 1651 (1991), and references therein.

[9] M. Wilkinson and E. J. Austin, Phys. Rev. B **50**, 1420 (1994), and references therein.

[10] M. C. Geisler, J. H. Smet, V. Umansky, K. von Klitzing, B. Naundorf, R. Ketzmerick, and H. Schweizer, Phys. Rev. Lett. **92**, 256801 (2004).

[11] P. Leboeuf, J. Kurchan, M. Feingold, and D. P. Arovas, Phys. Rev. Lett. **65**, 3076 (1990).

[12] R. Lima and D. Shepelyansky, Phys. Rev. Lett. **67**, 1377 (1991).

[13] T. Geisel, R. Ketzmerick, and G. Petschel, Phys. Rev. Lett. **67**, 3635 (1991).

[14] R. Artuso *et al.*, Int. J. Mod. Phys. B **8**, 207 (1994), and references therein.

[15] I. Dana, Phys. Rev. Lett. **73**, 1609 (1994).

[16] I. Dana, Phys. Lett. A **197**, 413 (1995).

[17] I. Dana, Phys. Rev. E **52**, 466 (1995).

[18] I. Dana, M. Feingold, and M. Wilkinson, Phys. Rev. Lett. **81**, 3124 (1998).

[19] I. Dana, Y. Rutman, and M. Feingold, Phys. Rev. E **58**, 5655 (1998).

[20] F. Faure, J. Phys. A **33**, 531 (2000).

[21] G. M. Zaslavskii, M. Yu. Zakharov, R. Z. Sagdeev, D. A. Usikov, and A. A. Chernikov, Zh. Eksp. Teor. Fiz. **91**, 500 (1986) [Sov. Phys. JETP **64**, 294 (1986)].

[22] I. Dana and M. Amit, Phys. Rev. E **51**, R2731 (1995).

[23] S. Pekarsky and V. Rom-Kedar, Phys. Lett. A **225**, 274 (1997).

[24] M. H. Johnson and B. A. Lippmann, Phys. Rev. **76**, 828 (1949).

[25] I. Dana, E. Eisenberg, and N. Shnerb, Phys. Rev. E **54**, 5948 (1996).

[26] R. M. Wilcox, J. Math. Phys. **8**, 962 (1967).

[27] The spectral width $\Delta E'(\pi)$ of $\hat{H}_{\text{eff}}/\epsilon$ can calculated exactly by diagonalizing a simple 2×2 matrix (A3) with (A4), while $\Delta E'(2\pi)$ is the width of the single band of $\hat{H}_{\text{eff}}/\epsilon = \hat{H}_1 + \epsilon\hat{H}_2 + \cdots$ for $\hbar = 2\pi$. Since $\epsilon = 0$ for $\hbar = 2\pi$, $\hat{H}_{\text{eff}}/\epsilon$ is exactly equal to $\hat{H}_1$, the Harper Hamiltonian (7) for which $\Delta E'(2\pi) = 4$, independent of μ.